

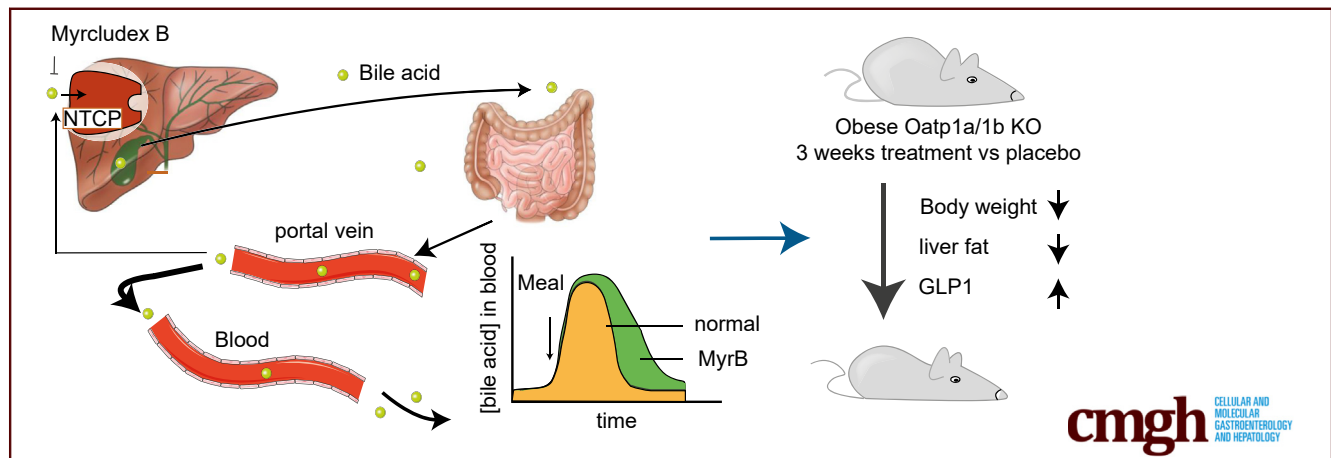
ORIGINAL RESEARCH

Inhibition of Hepatic Bile Acid Uptake by Myrcludex B Promotes Glucagon-Like Peptide-1 Release and Reduces Obesity



Joanne M. Donkers,¹ Reinout L. P. Roscam Abbing,¹ Michel van Weeghel,^{2,3} Johannes H. M. Levels,⁴ Anita Boelen,⁵ Alfred H. Schinkel,⁶ Ronald P. J. Oude Elferink,^{1,7} and Stan F. J. van de Graaf^{1,7}

¹Tytgat Institute for Liver and Intestinal Research, Amsterdam Gastroenterology Endocrinology Metabolism, Amsterdam University Medical Center, University of Amsterdam, Amsterdam, the Netherlands; ²Laboratory Genetic Metabolic Diseases, Amsterdam Gastroenterology Endocrinology Metabolism, Amsterdam University Medical Center, University of Amsterdam, Amsterdam, the Netherlands; ³Core Facility Metabolomics, Amsterdam University Medical Center, University of Amsterdam, Amsterdam, the Netherlands; ⁴Department of Experimental Vascular Medicine, Amsterdam University Medical Center, University of Amsterdam, Amsterdam, the Netherlands; ⁵Endocrinology Laboratory, Amsterdam University Medical Center, University of Amsterdam, Amsterdam, the Netherlands; ⁶Division of Pharmacology, the Netherlands Cancer Institute, Amsterdam, the Netherlands; and ⁷Department of Gastroenterology and Hepatology, Amsterdam Gastroenterology Endocrinology Metabolism, Amsterdam University Medical Center, University of Amsterdam, Amsterdam, the Netherlands



SUMMARY

Targeting the hepatic bile acid uptake transporter Na⁺ taurocholate co-transporting polypeptide with Myrcludex B temporarily elevates plasma levels of endogenous bile acids in mice and is a novel means to attenuate body weight gain, reduce liver and body fat mass, lower plasma cholesterol, and increase GLP-1 (glucagon-like peptide-1) secretion.

BACKGROUND & AIMS: Bile acids are important metabolic signaling molecules. Bile acid receptor activation promotes body weight loss and improves glycemic control. The incretin hormone GLP-1 and thyroid hormone activation of T4 to T3 have been suggested as important contributors. Here, we identify the hepatic bile acid uptake transporter Na⁺ taurocholate co-transporting polypeptide (NTCP) as target to prolong postprandial bile acid signaling.

METHODS: Organic anion transporting polypeptide (OATP)1a/1b KO mice with or without reconstitution with human

OATP1B1 in the liver were treated with the NTCP inhibitor Myrcludex B for 3.5 weeks after the onset of obesity induced by high fat diet-feeding. Furthermore, radiolabeled T4 was injected to determine the role of NTCP and OATPs in thyroid hormone clearance from plasma.

RESULTS: Inhibition of NTCP by Myrcludex B in obese Oatp1a/1b KO mice inhibited hepatic clearance of bile acids from portal and systemic blood, stimulated GLP-1 secretion, reduced body weight, and decreased (hepatic) adiposity. NTCP inhibition did not affect hepatic T4 uptake nor lead to increased thyroid hormone activation. Myrcludex B treatment increased fecal energy output, explaining body weight reductions amongst unaltered food intake and energy expenditure.

CONCLUSIONS: Pharmacologically targeting hepatic bile acid uptake to increase bile acid signaling is a novel approach to treat obesity and induce GLP1- secretion. (*Cell Mol Gastroenterol Hepatol* 2020;10:451–466; <https://doi.org/10.1016/j.jcmgh.2020.04.009>)

Keywords: NTCP; OATP; Myrcludex B; Obesity.

Bile acids facilitate the absorption of dietary fat and fat-soluble nutrients. Furthermore, they are recognized as potent signaling molecules activating a range of membrane and nuclear receptors located in- and outside the enterohepatic system, of which the farnesoid X receptor (FXR) (*NR1H4*) and the G protein-coupled bile acid receptor (GPBAR1 or TGR5) are the best studied. Activation of FXR and TGR5 has been shown to decrease body weight, improve glucose tolerance, and reduce inflammation in mice.¹⁻³ Importantly, these bile acid-induced effects are executed through downstream signaling processes, which are currently not completely understood. Increased energy expenditure via deiodinase 2 (Dio2)-mediated thyroid hormone activation⁴ and the incretin hormone GLP-1 (glucagon-like peptide-1)⁵⁻⁷ have been suggested as important contributors for bile acid-induced weight loss. Chronically targeting a single receptor is in contrast to the physiologic situation in which bile acid dynamics follow a meal-dependent rhythm,⁸ likely clarifying the appearance of side effects with the use of synthetic bile acid receptor agonists.⁹⁻¹¹ Therefore, we aimed to temporarily stimulate the signaling effects of endogenous bile acids to peripheral tissues by inhibiting hepatic bile acid uptake.

Bile acids undergo efficient enterohepatic cycling, with over 95% intestinal absorption and limited escape of bile acids from the portal vein into the systemic circulation.¹² The hepatic transporter sodium taurocholate co-transporting polypeptide (NTCP) (*SLC10A1*) functions as the main uptake transporter of conjugated bile acids, as was demonstrated in NTCP knockout (KO) mice¹³ and in humans with NTCP gene mutations.^{14,15} Recently, NTCP has been identified as the entry receptor for the hepatitis B virus (HBV) and hepatitis delta virus (HDV),^{16,17} and a peptide called Myrcludex B, interfering with NTCP-HBV interaction, is currently being tested in HBV/HDV clinical trials.¹⁸⁻²⁰ Myrcludex B also efficiently inhibits NTCP-mediated bile acid transport leading to a temporary increase in systemic bile acid levels in humans.¹⁸ Bile acid excursions in Myrcludex B-treated wild-type (WT) mice are largely absent, as they display efficient hepatic uptake of conjugated bile acids also by members of the organic anion transporting polypeptide (OATP) 1a/1b family,²¹ which were previously believed to mediate only the transport of unconjugated bile acid species.^{12,22} As Myrcludex B does create a temporary elevation in plasma bile acid levels in these Oatp1a/1b-deficient mice,²¹ they mimic the situation in humans after Myrcludex B administration. We employed this mouse model to investigate the metabolic impact of prolonged bile acid signaling after the onset of obesity.

We demonstrate that partial inhibition of hepatic bile acid clearance from the portal and systemic circulation reduces body weight and (hepatic) adiposity. Therefore, NTCP is a potential therapeutic target for the treatment of obesity or fatty liver disease.

Results

Prolonged Bile Acid Signaling by NTCP Inhibition Boosts GLP-1 Secretion

To evaluate the in vivo impact of bile acids on GLP-1 secretion, we used the NTCP inhibitor Myrcludex B to prolong bile acid signaling in obese Oatp1a/1b-deficient mice. Treatment with Myrcludex B was started 15 weeks after the onset of obesity by high-fat diet (HFD) feeding. In line with previous research,^{21,22} Oatp1a/1b KO mice display slightly elevated (unconjugated) bile acid levels compared with WT control animals (average WT 1.64 vs KO 6.13 μ M of total bile acids) (Figure 1A). Myrcludex B treatment profoundly increased levels of total and conjugated bile acids in Oatp1a/1b KO mice 3-4 hours after the Myrcludex B injection (Figure 1A). The increase in plasma bile acids was temporary, as they completely normalized within 24 hours after the injection.^{21,23} Inhibition of NTCP by Myrcludex B increased fasting GLP-1 levels 4-fold (Figure 1B). Next, we evaluated if the Myrcludex B-mediated GLP-1 increase affected glycemic control. HFD-fed Oatp1a/1b KO mice treated with Myrcludex B tended to have lower insulin levels before and 15 minutes after oral glucose administration (Figure 1C). Although this suggested improved insulin sensitivity upon Myrcludex B treatment, the responses to glucose and insulin tolerance tests were not different between HFD-fed Oatp1a/1b KO mice receiving placebo or Myrcludex B treatment (Figure 1D and E). As it was recently shown that GLP-1 signaling can increase thermogenesis in brown adipose tissue (BAT),²⁴⁻²⁷ we assessed body temperature using temperature transponders placed near the BAT. Body temperature in HFD-fed OATP1a/1b KO mice treated with Myrcludex B significantly increased with an average of 0.9°C, while body temperature of placebo-treated animals remained unchanged (Figure 1F). Messenger RNA expression of Ucp1 (uncoupling protein 1), a mitochondrial gene known for its central role in BAT thermogenesis,^{28,29} increased in BAT, suggesting increased thermogenesis in BAT of Myrcludex B treated HFD-fed OATP1a/1b KO mice (Figure 1G), but this increase was not observed at the protein level, and also, the UCP signal in subcutaneous white

Abbreviations used in this paper: ALP, alkaline phosphatase; BAT, brown adipose tissue; cAMP, adenosine 3',5'-cyclic monophosphate; Dio, deiodinase; ELISA, enzyme-linked immunosorbent assay; FCS, fetal calf serum; FXR, farnesoid X receptor; GTT, glucose tolerance test; HBV, hepatitis B virus; HDV, hepatitis delta virus; HFD, high fat diet; KO, knockout; NAFLD, nonalcoholic fatty liver disease; NTCP, sodium taurocholate co-transporting polypeptide; OATP, organic anion transporting polypeptide; PEPCK, Phosphoenolpyruvate carboxykinase; TC, taurocholic acid; TCDCA, taurochenodeoxycholic acid; TG, triglyceride; VLDL, very low-density lipoprotein; WT, wild-type.

 Most current article

© 2020 The Authors. Published by Elsevier Inc. on behalf of the AGA Institute. This is an open access article under the CC BY-NC-ND license (<http://creativecommons.org/licenses/by-nc-nd/4.0/>).

2352-345X

<https://doi.org/10.1016/j.jcmgh.2020.04.009>

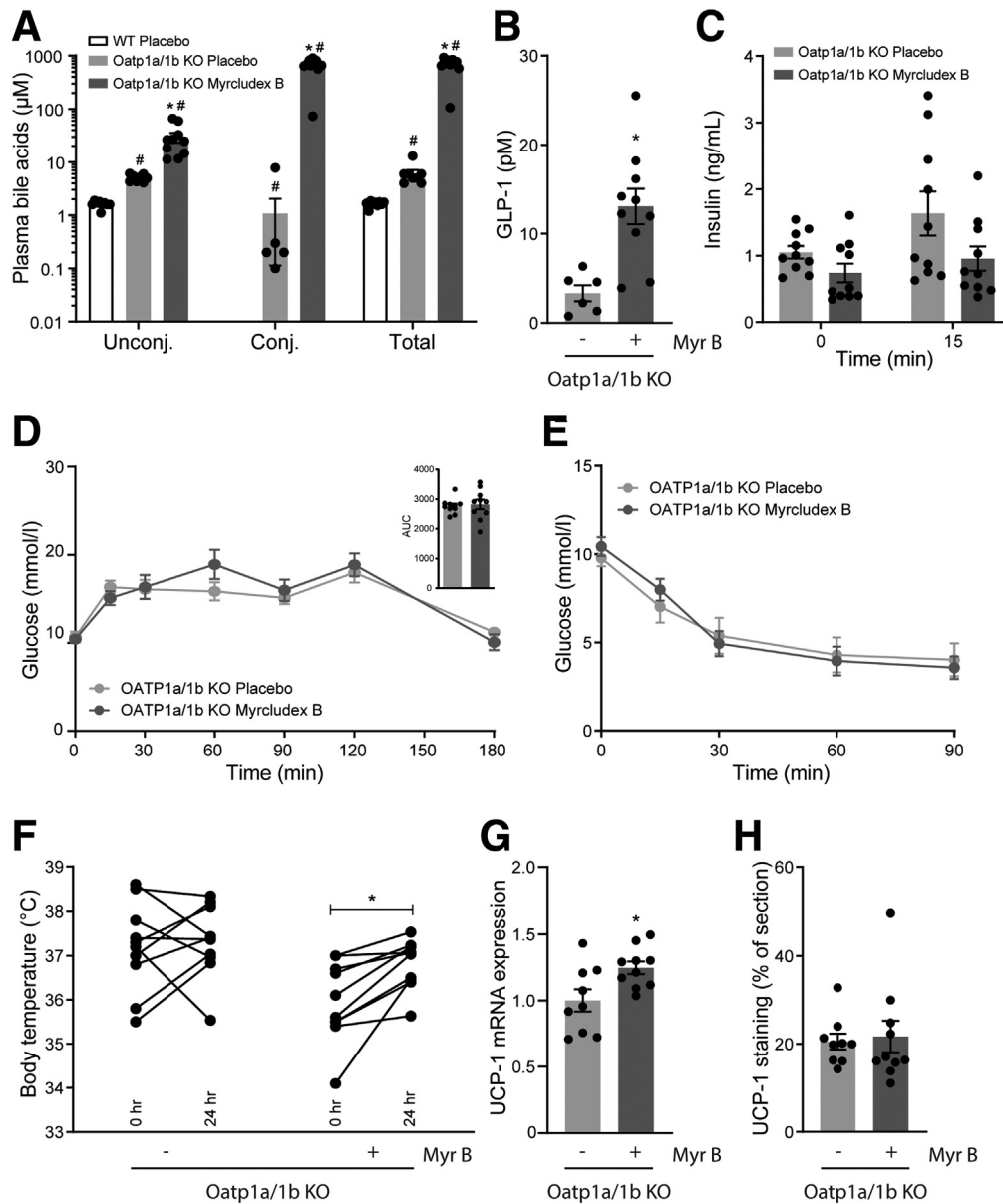


Figure 1. NTCP inhibition by Myrcludex B increases plasma bile acid and GLP-1 levels. (A) Unconjugated, conjugated, and total plasma bile acid levels 3 hours after placebo or Myrcludex B (2.5 µg/g) injection in male obese WT and *Oatp1a/1b* KO mice (n = 9–10). Mice were fed a HFD for 16 weeks and subsequently treated daily with placebo or Myrcludex B for 3.5 weeks. (B) Fasting GLP-1 levels and (C) plasma insulin levels (D) during an oral glucose tolerance test (2 g/kg glucose) and (E) an insulin tolerance test (1.2 mU/kg) of the *Oatp1a/1b* KO mice described in panel A. (F) Body temperature, measured by temperature transponders placed near the BAT of the mice in panel A. Per animal, average body temperature was calculated from 3 individual observations. (G) *Ucp1* messenger RNA expression levels, determined by reverse transcription quantitative polymerase chain reaction in BAT of the *Oatp1a/1b* KO mice described in panel A. Reverse transcription quantitative polymerase chain reaction samples are relative to the geometric mean of control genes *36b4* and *Hprt* and were normalized to the placebo treated group. (H) Quantified UCP-1 staining in sWAT of the *Oatp1a/1b* KO mice described in panel A. Error bars show SEM, asterisk indicates significant changes. AUC, area under the curve.

adipose tissue (sWAT) was not increased (Figure 1H), so “browning” of adipose tissue was not evident.

Infusion of Conjugated Bile Salt Also Stimulates GLP-1 Secretion

The pivotal role for high systemic conjugated bile acids in bile acid-stimulated GLP-1 secretion was supported by

an infusion challenge. As WT mice are very efficient in clearing bile acids from the systemic circulation,^{13,21} we also used NTCP KO animals with delayed hepatic bile acid transport,¹³ letting us more accurately study the effect of systemic conjugated bile acids. Constant intravenous infusion of taurocholic acid (TC), with increasing concentrations every 20 minutes, amplified GLP-1 release in WT animals, but much stronger effects were observed in

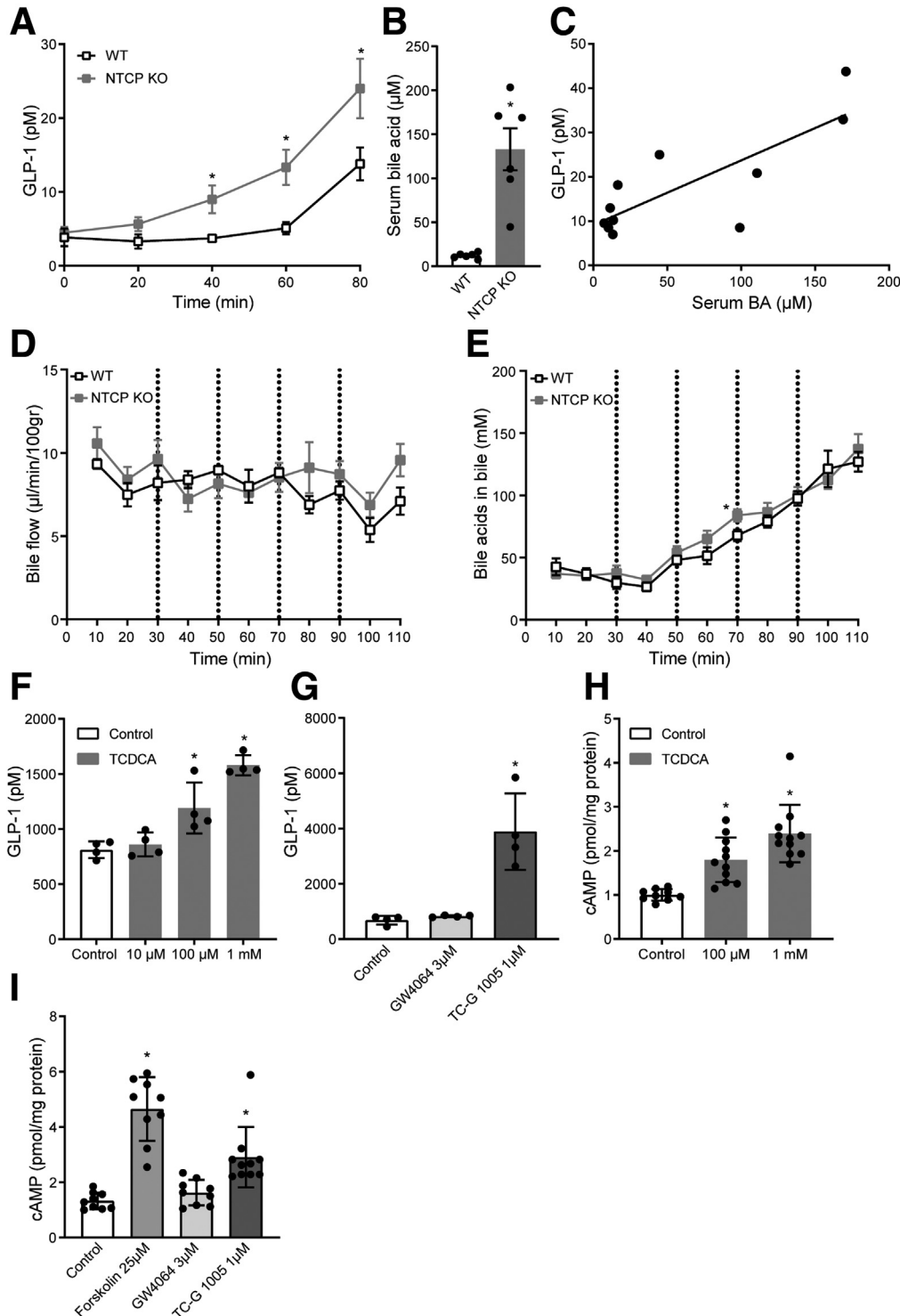


Figure 2. Conjugated bile acids stimulate GLP-1 secretion. (A) Plasma GLP-1 during and (B) total bile acids after the intravenous infusion of bile acid TC (150–600 nmol/min, 0.1- to 0.4-mL/h infusion rate) in WT or NTCP KO mice ($n = 10-12$). (C) Scatterplot showing the significant correlation between plasma levels of GLP-1 (y-axis) and bile acids (x-axis). Values are determined at the last time point in the TC intravenous infusion experiment. (D) Bile flow and (E) bile acid concentration in bile during the intravenous infusion of bile acid TC (150–600 nmol/min, 0.1- to 0.4-mL/h infusion rate) in WT or NTCP KO mice ($n = 10-12$). (F) GLP-1 secretion of GLUTag cells after a 2-hour treatment with bile acid TCDCA or (G) TGR5 agonist TC-G 1005 and FXR agonist GW4064 (representative results of 3 independent experiments, $n = 4$ wells/group). Two-minute cAMP secretion of GLUTag cells treated with (H) TCDCA or (I) TC-G 1005, GW4064, or positive control forskolin. Samples were normalized to protein content, results of 3 independent experiments ($n = 9-11$). Error bars show (A–E) SEM or (F–I) SD. Asterisk indicates significant changes compared with the control group.

NTCP-deficient mice (Figure 2A). Delayed hepatic clearance of the extra infused conjugated bile acids in the latter group was demonstrated by a 11.1 ± 2.0 -fold higher plasma bile acid concentration at the end of the experiment (Figure 2B), and correlation analysis suggested a direct effect of the increase in systemic conjugated bile acids on GLP-1 secretion (Figure 2C). Bile flow and the concentration of bile acids in bile were not

different between the groups (Figure 2D and E). Next, we used the established GLP-1 secreting enteroendocrine L-cell line (GLUTag) to study the potential receptor pathway. The conjugated bile acid taurochenodeoxycholic acid (TCDCA) promotes GLP-1 release ~2-fold compared with unstimulated control cells (Figure 2F). Similarly, the synthetic TGR5 agonist TC-G 1005 increased GLP-1 secretion, while FXR agonism using GW4064 did not

elicit any response (Figure 2G). We also analyzed intracellular adenosine 3',5'-cyclic monophosphate (cAMP) levels, using forskolin as a positive control. Both the bile acid TCDCa and the TGR5 agonist TC-G 1005, but not the FXR agonist GW4064, significantly increased intracellular cAMP levels (Figure 2H and I). Collectively, these results suggest that overflow of conjugated bile acids into the systemic circulation stimulates cAMP-driven GLP-1 secretion, likely targeting TGR5 in intestinal L-cells from the basolateral (blood-facing) side.

OATPs But Not NTCP Play a Role in T4 Transport

Increased bile acid signaling has been linked to increased intracellular thyroid hormone activation in BAT.⁴ Thyroid hormones, once taken up in the cell by specific transporters, can be metabolized by deiodinases, an enzyme family consisting of 3 types: type 1 (Dio1), type 2 (Dio2), and type 3 (Dio3).³⁰ Dio1, highly expressed in the liver, and Dio2, among others localized in the BAT, convert T4 into the biologically active T3, while Dio3 is the major thyroid hormone-inactivating enzyme.³¹ Prolonged bile acid signaling in Myrcludex B-treated, HFD-fed Oatp1a/1b KO mice created a trend toward increased *Dio2* gene expression in BAT, while OATP deficiency itself did not alter *Dio2* expression levels (Figure 3A). As OATPs can also transport thyroid hormones,^{22,32,33} we evaluated plasma T3 and T4 and noted that OATP deficiency results in T3 levels below and T4 levels above the WT control animals (Figure 3B and C). Myrcludex B treatment seems to enlarge these differences even further, particularly decreasing plasma T3 levels. The conversion of T4 to T3 by Dio1 in the liver largely controls the circulating T3 levels.³⁴ *Dio1* gene expression was downregulated in OATP-deficient mice, and the decrease was further augmented after Myrcludex B treatment (Figure 3D). As NTCP has been proposed to contribute to hepatic thyroid hormone uptake, and impaired hepatic T4 uptake would explain the observed reduced T3 and Dio1 levels,³⁴ we determined the capacity of OATPs and NTCP to transport T4. Altered transport of T3 upon inhibition of NTCP is unlikely, as it was shown that NTCP is not critical for the transport of a T3 analogue in mice.³⁵ The T4 clearance rate from the plasma was 2.3-fold decreased in Oatp1a/1b KO mice compared with WT control animals, unaffected by sex (Figure 3E and F). Decreased accumulation of T4 in the bile and liver of OATP-deficient mice closely follows the decreased plasma clearance (Figure 3G and H). Inhibition of NTCP by Myrcludex B had no additional effects on plasma clearance in either WT or Oatp1a/1b KO mice (Figure 3E and F). The OATP1B subfamily of OATP proteins has previously been suggested to play a dominant role in thyroid hormone transport in mice and humans.³² Therefore, we studied if the human OATP isoforms OATP1B1 and OATP1B3 could restore T4 transport in OATP-deficient mice. Transgenic expression of human OATP1B1, but not human OATP1B3, in Oatp1a/1b null mice (called Oatp1a/1b KO-h1B1 and Oatp1a/1b KO-h1B3 mice, respectively) largely restored the T4 plasma clearance rate to control levels (Figure 3F). In line with these findings, we confirmed

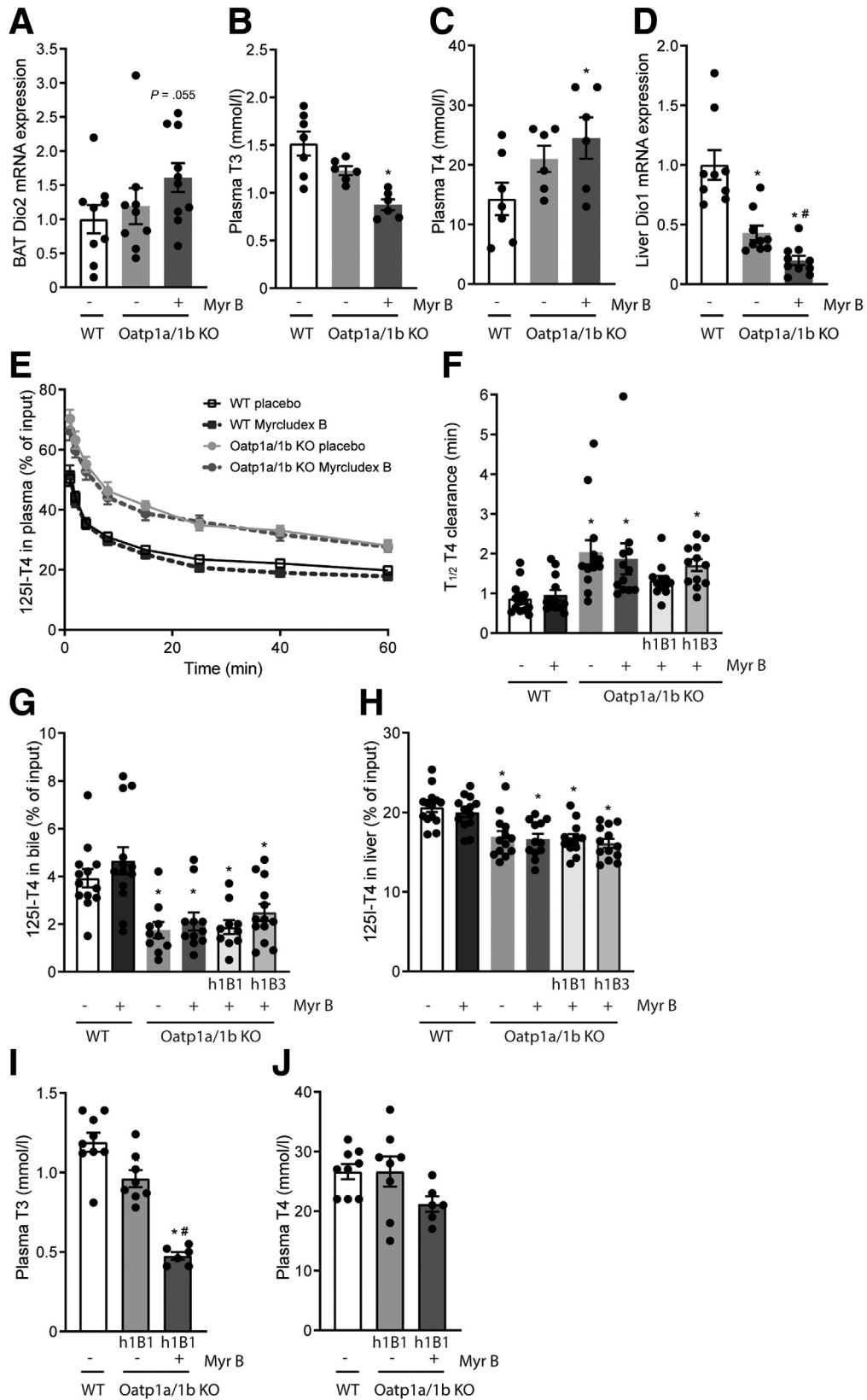
normalization of plasma T4 in HFD-fed Oatp1a/1b KO-h1B1 mice treated with Myrcludex B, and T3 levels remained only slightly reduced (Figure 3I and J). Therefore, we next used Oatp1a/1b KO-h1B1 mice to study the effects of Myrcludex B-induced bile acid excursions on metabolic parameters.

Pharmacological Inhibition of NTCP Reduces Body Weight and Hepatic Steatosis

Daily prolonged elevated plasma bile acid levels by Myrcludex B administration for 3.5 weeks rapidly reduced body weight in HFD-fed Oatp1a/1b KO-h1B1 mice (Figure 4A and B). In parallel with the reduction in body weight, Myrcludex B treatment significantly reduced fat mass, mainly in the subcutaneous compartment (Figure 4C). Furthermore, histopathology of the liver indicated reduced steatosis in the treated animals (Figure 4D, quantified in Figure 4E). Glucose areas under the curve upon glucose or insulin administration (glucose tolerance test [GTT]/insulin tolerance test) were not significantly affected by Myrcludex B treatment in Oatp1a/1b KO-h1B1 mice, whereas insulin was reduced and GLP-1 levels increased 15 minutes after oral glucose administration (Figure 4F and G). Daily Myrcludex B treatment in WT mice does not lead to bile acid excursions and did not affect body weight during the 10-week treatment period (Figure 5A), suggesting that the Myrcludex B-induced body weight loss in Oatp1a/1b KO-h1B1 mice was not a consequence of drug toxicity but was related to bile acid elevations. Furthermore, Myrcludex B treatment did not lead to liver damage in Oatp1a/1b KO-h1B1 mice, as liver enzymes were mostly unchanged. Only for alkaline phosphatase (ALP) a very modest elevation was detected (Figure 5B). Of note, this increase in ALP for Myrcludex B treated HFD-fed Oatp1a/1b KO-h1B1 mice is a factor of 10 lower compared with those measured by us in mice with cholestatic liver damage.³⁶ No differences in Ki-67 staining were observed (Figure 5C), which is a marker for regeneration upon liver damage. Similarly, Sirius red staining on liver sections did not reveal any signs of fibrosis, in contrast to the positive control which were cholestatic mice (cholate-fed *Mdr2* KO) (Figure 5D). Additionally, no changes were observed in mRNA levels for fibrotic markers α -SMA and Col1a1, and inflammatory markers MCP-1 and TGF- β (Figure 5E).

NTCP Inhibition Stimulates Fatty Acid Oxidation and Fecal Energy Excretion

To explain the weight improvements of the animals treated with Myrcludex B, we measured food intake and fecal energy excretion. Furthermore, we assessed ambulatory activity and total energy expenditure. Myrcludex B treatment did not affect the food intake of Oatp1a/1b KO-h1B1 mice (Figure 6A). However, the elevated energy content in the feces of Myrcludex B-treated Oatp1a/1b KO-h1B1 animals pointed toward decreased caloric extraction from the diet (Figure 6B). Indirect calorimetry was performed on chow-fed mice of equal body weight to prevent biased observations due to body weight and fat



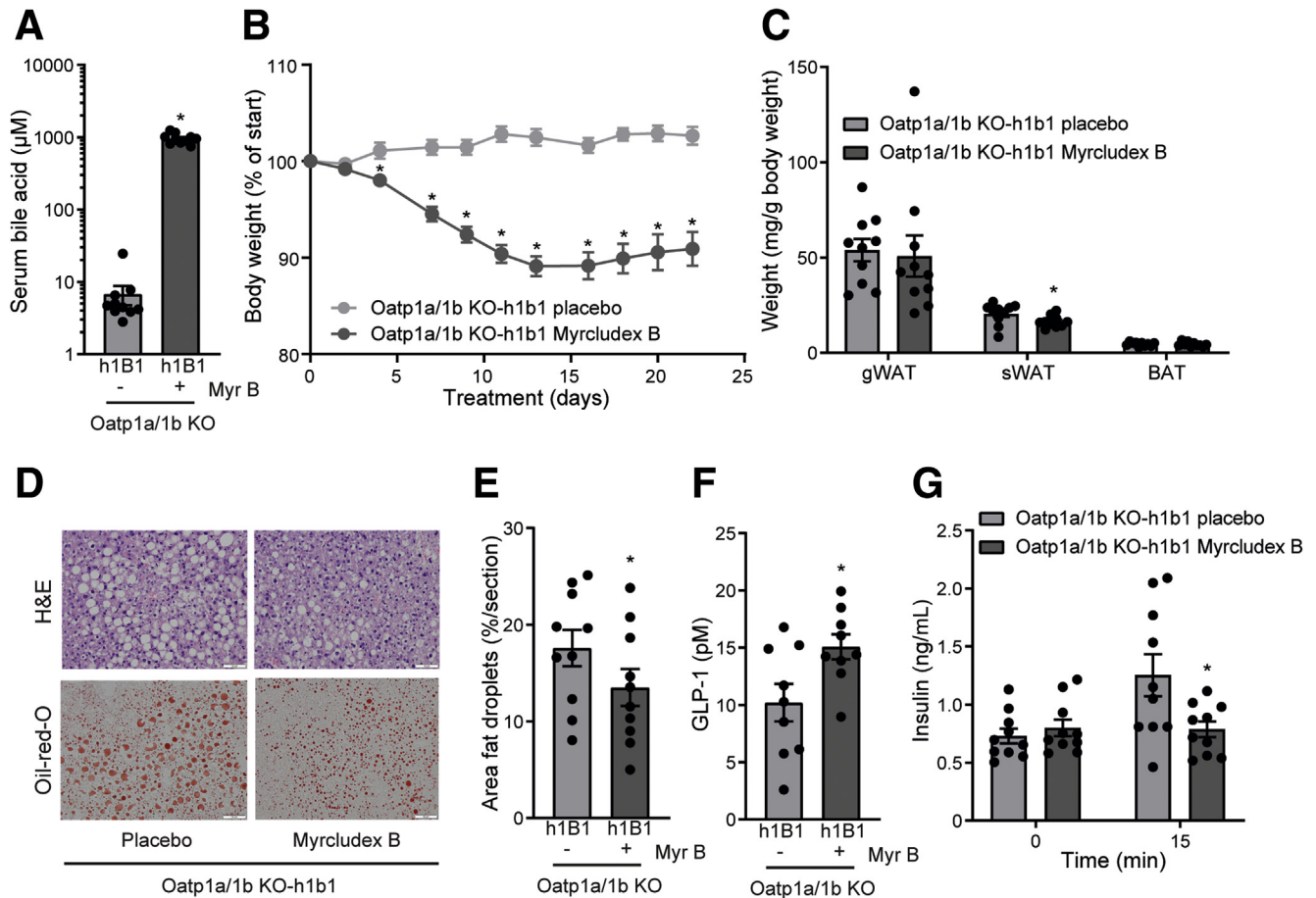


Figure 4. Prolonged bile acid signaling by NTCP inhibition reduces body weight and adiposity in obese mice. Total plasma bile acid levels 3 hours after placebo or Myrcludex B (2.5 $\mu\text{g/g}$) injection and after (A) a 4- to 5-hour fast, (B) body weight change, and (C) adipose tissue weights of female HFD-fed Oatp1a/1b KO-h1B1 mice treated daily with placebo or Myrcludex B for 3.5 weeks ($n = 10$). (D) Hepatic TG content by representative images of liver histology by hematoxylin and eosin (H&E) (top) and Oil Red O (bottom) staining and (E) quantified Oil Red O staining ($n = 4$ images/mouse, 10 mice/group). (F) Fasting plasma GLP-1 levels and (G) plasma insulin levels, 0 and 15 minutes after an oral glucose bolus (2 g/kg) of the mice described in panel A. Error bars show SEM, asterisk indicates significant changes. gWAT, gonadal white adipose tissue; sWAT, subcutaneous white adipose tissue.

mass differences between long-term Myrcludex B or placebo treated HFD-fed mice. Locomotor activity and total energy expenditure were not changed upon Myrcludex B treatment (Figure 6C and D), but the respiratory quotient demonstrates an immediate switch toward fat oxidation right after Myrcludex B injection (Figure 6E), which

correlates with the Myrcludex B-mediated temporary increase in plasma bile acid levels. Pharmacological inhibition of NTCP significantly reduced plasma cholesterol in HFD-fed Oatp1a/1b KO mice (Figure 6F) while plasma triglycerides (TG) were relatively increased (Figure 6G). Note that the TG levels did not exceed levels observed in

Figure 3. (See previous page) OATPs but not NTCP transport T4. (A) *Dio2* messenger RNA (mRNA) expression levels in BAT of male HFD-fed Oatp1a/1b KO mice treated daily with placebo or Myrcludex B for 3.5 weeks ($n = 9-10$). Reverse transcription quantitative polymerase chain reaction samples are relative to the geometric mean of control genes *36b4* and *Hprt* and normalized to reference values of male WT HFD-fed placebo treated mice. (B) Plasma T3 and (C) plasma T4 levels of the mice described in panel A. (D) *Dio1* mRNA expression levels in the liver, reverse transcription quantitative polymerase chain reaction samples are relative to the geometric mean of control genes *36b4* and *tbp* and normalized to reference values of male WT HFD-fed placebo treated mice. (E) T4 signal in plasma and (F) half-life of the T4 plasma clearance in WT, Oatp1a/1b KO, or Oatp1a/1b KO reconstituted with human OATP1B1 or OATP1B3 (Oatp1a/1b KO-h1B1 or Oatp1a/1b KO-h1B3) after Myrcludex B or placebo administration ($n = 13-14$, equal male and female animals). [^{125}I]T4 was administered intravenously via the tail vein at $t=0$ and [^{125}I] activity (cpm) was measured. Appearance of radiolabeled T4 in (G) bile and (H) the liver. Data are expressed as percentage of input. (I) Plasma T3 and (J) plasma T4 levels of female HFD-fed WT and Oatp1a/1b KO-h1B1 mice treated daily with placebo or Myrcludex B for 3.5 weeks ($n = 9-10$). Error bars show SEM, asterisk indicates significant changes to the placebo treated control group, hashtag indicates significant changes to the placebo treated Oatp1a/1b KO(-h1B1) group.

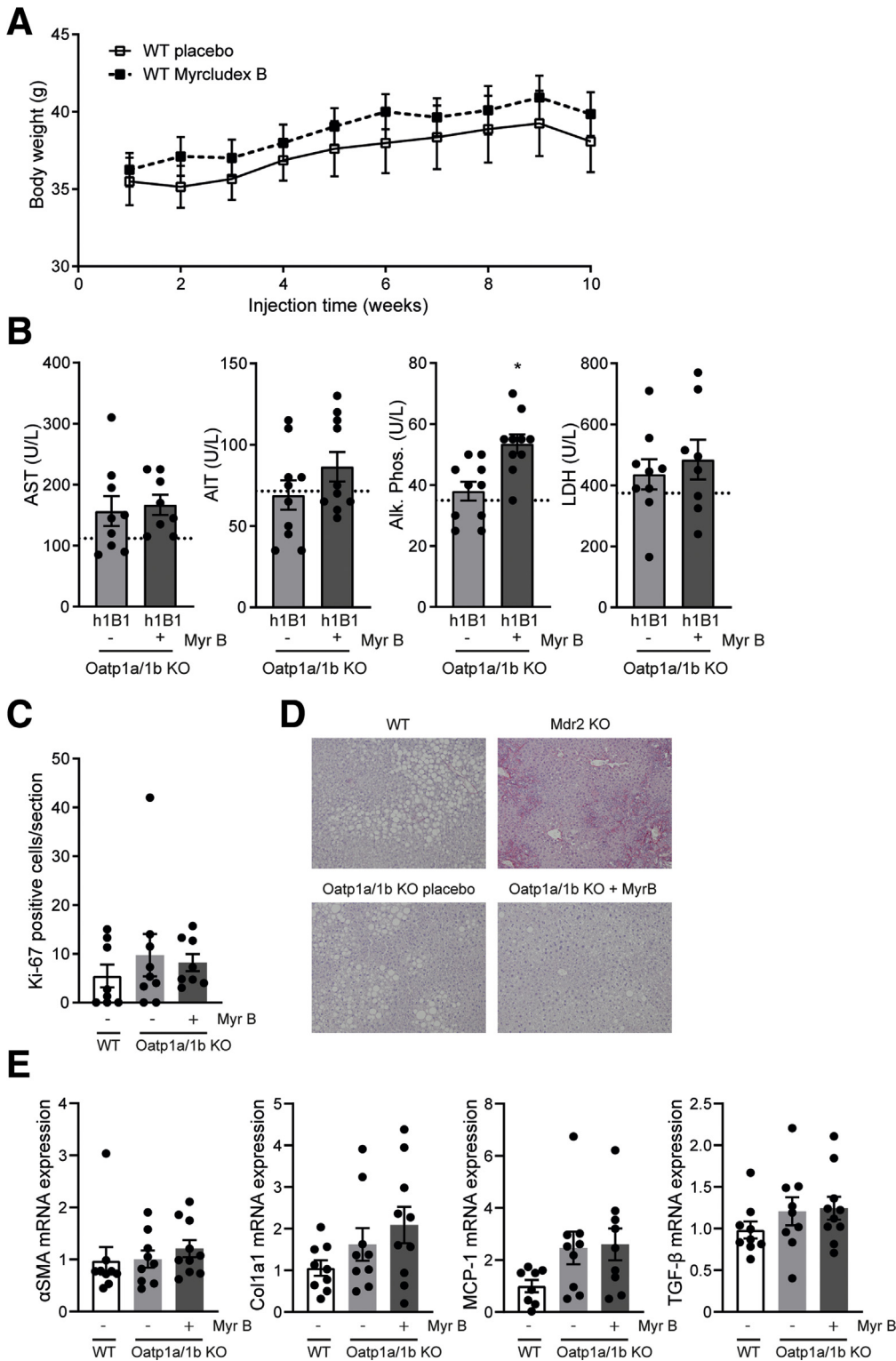
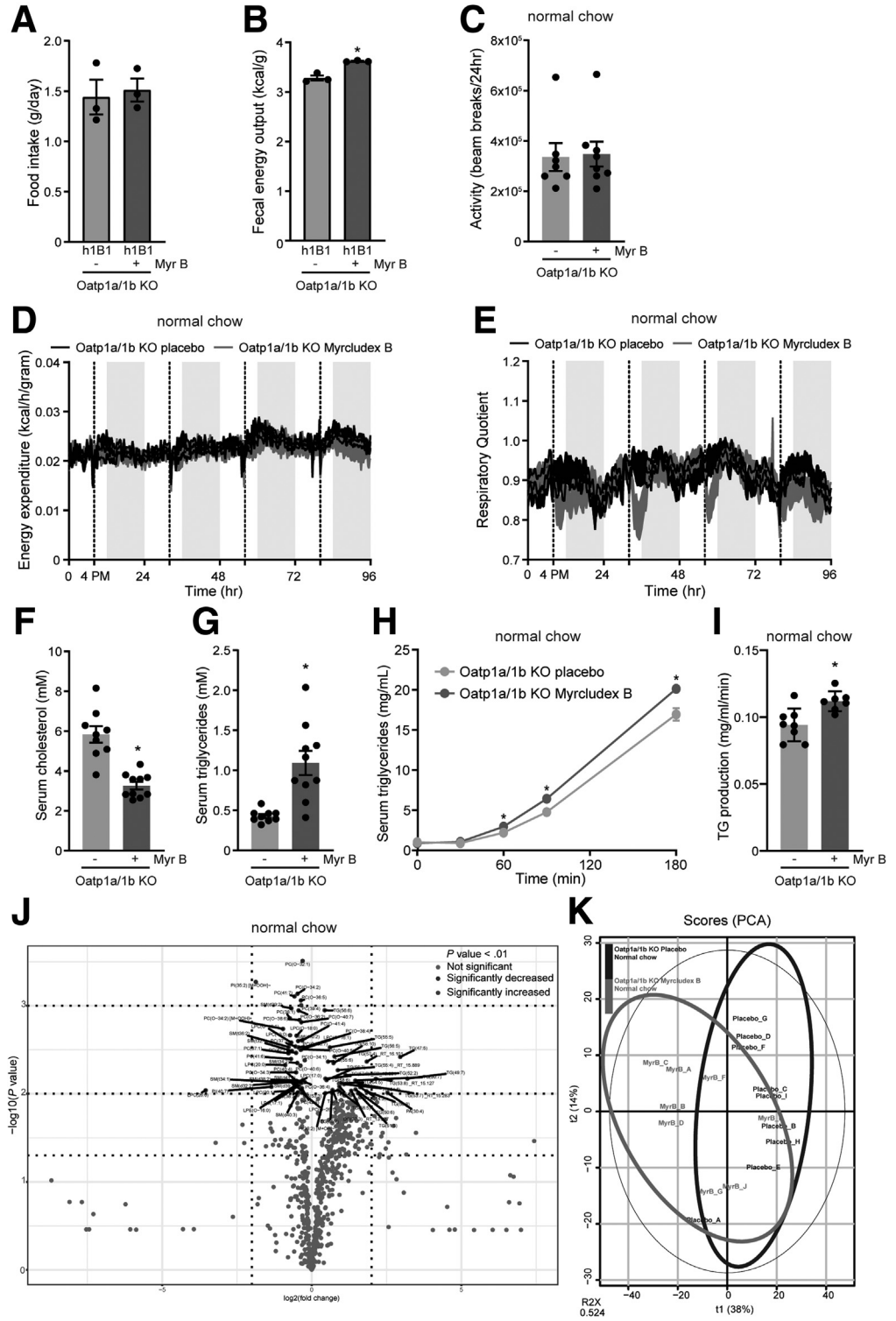


Figure 5. Safety aspects of Myrcludex B. (A) Myrcludex B treatment for 10 weeks does not affect body weight of obese male C57Bl/6 WT mice (n = 11–12). (B) Comparison of plasma aspartate aminotransferase (AST), alanine aminotransferase (ALT), ALP, and lactate dehydrogenase (LDH) of HFD-fed female Oatp1a/1b KO-h1B1 mice treated with placebo or Myrcludex B for 3.5 weeks. Reference values of placebo treated WT HFD mice are indicated with dashed lines. (C) Quantification of amount of Ki-67 positive cells in liver sections of male HFD-fed WT or Oatp1a/1b KO mice treated daily with placebo or Myrcludex B for 3.5 weeks (n = 9–10) (n = 4 images/mouse). (D) Representative images of liver morphology using Sirius red as fibrotic marker. As positive control, a liver of a fibrotic Mdr2-deficient cholate-fed mouse was included. (E) α SMA, Col1a1, MCP-1, and TGF- β messenger RNA expression levels in livers of male HFD-fed Oatp1a/1b KO mice treated daily with placebo or Myrcludex B for 3.5 weeks (n = 9–10). Reverse transcription quantitative polymerase chain reaction samples are relative to the geometric mean of control genes *36b4* and *Hprt* and normalized to reference values of male WT HFD-fed placebo treated mice. Error bars show SEM, asterisk indicates significant changes.

control chow fed mice (1.1 ± 0.15 mM for HFD-fed Myrcludex B-treated OATP1a/1b KO mice vs 1.3 ± 0.16 mM for chow-fed control mice). This relative increase possibly originates from an increased peripheral TG need that drives a moderately increased hepatic very

low-density lipoprotein (VLDL)-TG secretion rate, as was shown for fasted Oatp1a/1b KO mice after Myrcludex B injection (Figure 6H and I). Alternatively, the elevated bile salt levels could dampen hepatic TG uptake.³⁷ Unbiased lipidomics, to further investigate

Figure 6. NTCP inhibition by Myrcludex B stimulates fatty acid oxidation, stimulates fecal energy excretion, and mobilizes VL/L-derived TG. (A) Food intake of HFD-fed female KO-h1B1 mice during their daily treatment with placebo or Myrcludex B for 3.5 weeks. (B) Bomb calorimetry–assessed remaining calories in the feces of HFD-fed female Oatp1a/1b KO-h1B1 mice (n = 3). (C) Locomotor activity, (D) energy expenditure, and (E) respiratory quotient of chow-fed Oatp1a/1b KO mice, treated with placebo or Myrcludex B (2.5 μg/g), housed in calorimetric cages. Dashed line, 4PM, indicates injection with placebo or Myrcludex B (n = 8, crossover design). (F) Plasma cholesterol and (G) TG in male HFD-fed Oatp1a/1b KO mice treated daily with placebo or Myrcludex B for 3.5 weeks (n = 9–10). Hepatic VLDL secretion, determined after Poloxamer-407 (1 mg/kg) injection, measured by (H) serum TG accumulation and (I) calculated TG production rate (n = 7–8) in chow-fed Oatp1a/1b KO mice after Myrcludex B or placebo administration. (J) Volcano plot depicting the lipidomics data. Significance cutoff is shown in the legend (n = 8–9 mice per group, mice were treated with Myrcludex B for 5 consecutive days). (K) Principal component analysis (PCA) of the lipidomics analysis. Error bars show SEM, asterisk indicates significant changes.



individual lipid species, did not reveal a distinct plasma lipid subset that was elevated in Myrcludex B treated Oatp1a/1b KO mice compared with placebo-treated animals (Figure 6J and K). Lipidomics analysis identified changes in certain specific TG and (lyso)phosphatidylcholines, but no group of lipids was significant

different upon correction for multiple comparisons with the Holm-Sidak method.

Discussion

Here, we present the hepatic bile acid transporter NTCP as a novel pharmacological target to prolong bile acid presence

in peripheral tissues and blood and thereby counteract obesity and diet-induced fatty liver disease. These results complement to our recent study showing that NTCP KO mice are protected against obesity and hepatosteatosis when fed a HFD.³⁸ Prolonged elevated levels of endogenous bile acids more closely follows the natural situation in which postprandial increases in plasma bile acid levels temporarily target their receptors.⁸ As elevations in bile acid levels are positively linked to body weight loss after bariatric surgery,³⁹ increased bile acid signaling via inhibition of hepatic bile acid uptake could eventually contribute to new nonsurgical alternative treatments against obesity and obesity-related metabolic dysfunctions. Notably, elevated bile acid levels in mice and pigs after bariatric surgery were accompanied by reduced NTCP expression.^{40,41} Inspired by the fact that bariatric surgery also increases circulating GLP-1 levels,^{42,43} we assessed if this could be correlated to increased bile acid signaling. Our data demonstrates that increased conjugated bile acid levels resulted in pronounced effects on GLP-1 release in our models. Furthermore, the intravenous infusion of taurocholate supports that the bile acid-induced release of GLP-1^{44,45} occurs via stimulation of bile acid receptors at the basolateral side of the intestinal L-cell.⁴⁶ Despite significantly increased GLP-1 levels, glycemic control was not improved in the Myrcludex B-treated obese OATP1a/1b KO mice. The reason is not clear but factors such as decreased intestinal FXR-Fgf15 or hepatic FXR-PEPCK signaling, resulting from the temporary limited availability of bile salts in the small intestine and liver as a consequence of Myrcludex B-inhibited hepatic bile salt uptake, might counteract beneficial consequences of GLP-1 on glucose homeostasis.^{47–50} Furthermore, increased GLP-1 secretion is not observed in NTCP KO mice (WT HFD 6.41 ± 0.84 vs NTCP KO HFD 6.70 ± 1.06), unless they are continuously infused with bile salts (Figure 2A). This suggests that GLP-1 does not play a major role in the beneficial effects of NTCP inhibition on body weight reduction, as NTCP KO mice are also largely protected against detrimental effects of HFD. Increased energy loss via the feces clarified the negative energy balance, and thus body weight loss, in our mice treated with Myrcludex B. This may be related to the temporarily limited availability of bile acids in the small intestine, which then can alternate fat absorption, closely following observations in cholestatic and bile-deficient animals with lower intestinal bile acids.^{51,52} The temporary decrease in intestinal bile acids did not lead to (essential) fat malabsorption, as the lipidomics analysis did not indicate differences in plasma lipid profile after Myrcludex B treatment. A negative energy balance is a major driver for fat loss, as stored TG are used to compensate decreased food-derived energy substrates.⁵³ This is reflected in this study by decreased hepatic and sWAT TG content and enhanced lipolysis by peripheral tissues can explain the small increase in plasma TG, which we show is further enhanced by hepatic VLDL-TG secretion, possibly contributing to the lowering of hepatosteatosis. Finally, inhibition of the hepatic fatty acid uptake transporter FATP5 by elevated bile salt levels³⁷ could contribute as well.

NTCP KO mice at ~5 weeks of age fed a HFD display increased energy expenditure, linked to BAT activation

and likely contributing to the dampened body weight gain observed in these mice.³⁸ Unexpectedly, increased energy expenditure was not observed in Myrcludex B-treated Oatp1a/1b KO mice. The latter did show an acute drop in respiratory quotient, reflecting a shift toward lipid as preferred energy carrier for oxidative phosphorylation and thermometer transponders close to BAT registered an increase in body temperature. Although it remains unclear whether this discrepancy is due to differences in age, strain, or experimental setup (prevention vs treatment of obesity), the effectivity of targeting NTCP to lower body weight and hepatosteatosis is shown in both studies.

Safety of our strategy to prolong bile acid signaling by NTCP inhibition is illustrated by absence of adverse event in humans with NTCP gene mutations^{14,15} or after long-term Myrcludex B treatment of healthy volunteers, or even patients with chronic HBV/HDV infections.^{18,20,54,55} Furthermore, serious side effects previously reported for FXR and TGR5 activation by synthetic agonists, such as increased low-density lipoprotein cholesterol, pruritis,⁵⁶ and cell proliferation,^{57,58} are neither observed here in mice nor in Myrcludex B-treated patients.^{18,20,54,55} In fact, the mice demonstrate lower plasma cholesterol levels, which is likely a consequence of increased biliary cholesterol secretion as NTCP inhibition shifts bile salt uptake from periportal to pericentral hepatocytes.⁵⁹ With the emerging interest of the virology field to treat hepatitis B and delta co-infected patients with the NTCP inhibitor Myrcludex B, its transition to clinical practice is accelerated.^{18,20,54,60,61} Although clinical data on parameters such as body weight, fat mass, plasma glucose, GLP-1, and plasma TG still have to be elucidated, drug safety and the observed temporary increase in serum-conjugated bile acids, similar to our treated mice, makes Myrcludex B an interesting candidate drug to treat obesity and obesity-related metabolic dysfunctions in humans.

In conclusion, targeting the hepatic bile acid uptake transporter NTCP to prolong elevated levels of endogenous bile acids in plasma is a novel means to attenuate body weight gain, reduce liver and body fat mass, lower plasma cholesterol, and increase GLP-1 secretion.

Materials and Methods

Access to Data

All authors had access to the study data and had reviewed and approved the final paper. All the raw data files will be made available upon reasonable request.

Animals and Experimental Design

Oatp1a/1b KO mice (FVB background, Slco1a/1b cluster: *slco1a1*, *slco1a4*, *slco1a5*, *slco1a6*, *slco1b2*)²² and Oatp1a/1b knockouts reconstituted with liver-specific expression of human OATP1B1 or OATP1B3 and wild-type FVB control animals were obtained from Taconic Biosciences (Silkeborg, Denmark) (HFD experiments) or from the Netherlands Cancer Institute (Amsterdam, the Netherlands) (T4 clearance study). NTCP-deficient mice (*Slc10a1* KO, C57Bl/6 background)¹³ were bred in the Academic Medical Center

(Amsterdam, the Netherlands). Control WT C57Bl/6J Δ OlaHsd mice were purchased from Envigo (Horst, the Netherlands). Experiments were performed at the Academic Medical Center (Amsterdam, the Netherlands). Animals were co-housed with 3–4 animals and kept on a continuous 12-hour light/dark cycle (7:00–19:00) with ad libitum access to food and water. For the calorimetric studies, animals were individually housed in PhenoMaster cages (TSE Systems, Bat Homburg vor der Höhe, Germany). Energy expenditure data were corrected for body weight. Respiratory quotient was calculated as amount of CO₂ produced divided by the amount of O₂ consumed. Animals were fed a standard rodent chow, HFD (D12492; rodent diet with 60 kcal% fat; Research Diets, New Brunswick, NJ) or matching low-fat diet (D12450B; rodent diet with 10 kcal% fat; Research Diets). Female and male mice were 3–4 weeks old at the start of the HFD experiments, and for other experiments, mice were 8–12 weeks old. Myrcludex B (2.5 μ g/g body weight) was injected subcutaneously. Body weight was monitored twice weekly and food intake once weekly. Animal temperature data was obtained by noninvasively read-out of IPTT-300 temperature transponders (Bio-Medic Data Systems, Seaford, DE) subcutaneously implanted in the flank of the animal. Temperature was measured before and 24 hours after Myrcludex B or placebo injection. Glucose and insulin tolerance testing were performed 1 week before sacrifice. At the end of the study, a fasting (4–5 hours) blood sample was taken, and organs were harvested to be frozen in liquid nitrogen or formalin fixed. The study design and animal care and handling were approved by the Institutional Animal Care and Use Committee of the University of Amsterdam.

Chemicals

Bile acids TC and TCDCA, synthetic FXR-agonist GW4064, and Poloxamer 407 were purchased from Sigma-Aldrich (Zwijndrecht, the Netherlands). Synthetic TGR5-agonist TC-G 1005 was purchased from Tocris Bioscience (Abingdon, United Kingdom). Myrcludex B was synthesized by Pepsan (Lelystad, the Netherlands). D-glucose was obtained from Merck (Darmstadt, Germany), human insulin (humulin R U-100) was obtained from Lilly (Utrecht, the Netherlands), and sitagliptin phosphate monohydrate was purchased from BioVision (Milpitas, CA). [¹²⁵I]Thyroxine (T₄) (1080–1320 μ Ci/ μ g) (NEX111H100UC) was purchased from Perkin Elmer (Groningen, the Netherlands).

Glucose and Insulin Tolerance Testing

Animals fasted for 4–5 hours and received Myrcludex B or placebo injection 3 hours prior to the experiment. Mice received glucose (2 g/kg) by oral gavage or insulin (1.2 mU/kg) by intraperitoneal injection. Blood was drawn by the tail vein at 0, 15, 30, 60, and 90 minutes, and for the oral GTT also at 120 and 180 minutes. Glucose levels were determined in whole blood using a Contour XT glucometer (Bayer BV, Mijdrecht, the Netherlands). Blood collection for the insulin measurements occurred during the oral GTT. At 0 and 15 minutes, blood was

collected by vena saphena puncture and samples were kept at -80°C until measurement by Ultra Sensitive Mouse Insulin enzyme-linked immunosorbent assay (ELISA) kit (Crystal Chem, Elk Grove Village, IL) following the manufacturers' instructions.

Taurocholate (TC) Infusion

Male C57Bl/6J Δ OlaHsd and NTCP KO mice of 7–9 weeks of age were used for this experiment. Animals were fasted 4–5 hours prior to the experiment, and received an oral gavage with sitagliptin (25 mg/kg). Next, animals were anesthetized with an initial dose of saline containing ketamine (100 mg/mL) and xylazine (20 mg/mL), and maintained anesthetized using a saline-ketamine (100 mg/mL) solution. In the absence of a response to pain, the abdominal cavity was opened. The gall bladder was cannulated and bile was collected after distal ligation of the common bile duct, as described.^{13,62} Bile was continuously collected at 10-minute intervals. During the 30-minute bile depletion period, a second and third cannula were inserted in the arteria carotica communis and vena jugularis for blood collection and TC infusion, respectively. TC (150 nmol/min) was infused using a syringe pump 11 plus (Harvard Apparatus, Holliston, MA) using an infusion rate of 0.1 mL/h, increasing every 20 minutes with 0.1 mL/h, to a final TC infusion rate of 600 nmol/min. Blood for GLP-1 plasma measurements was collected before TC infusion started and every 20 minutes just before increasing the TC dosage. Blood was collected in EDTA-coated capillary tubes (Sarstedt, Newton, NC). Samples were centrifuged at 2000 rpm, 4°C for 10 minutes and plasma was transferred to clean Eppendorf tubes. Samples were kept at -80°C until measurement of active GLP-1 and insulin by ELISA (using EGLP-35K [Merck Millipore, Burlington, MA]) following the manufacturers' instructions. Eighty minutes after TC infusion, the experiment was terminated by switching off the pump followed by heart puncture of the animal.

Hepatic VLDL Secretion

Adult (>8 weeks old) male Oatp1a/1b KO mice were fasted 4–5 hours, after which they received an intravenous injection with Myrcludex B (2.5 μ g/kg) or placebo and an intraperitoneal injection with Poloxamer 407 (1 mg/kg). The next 3 hours, blood was sampled via the tail vein and TG were measured using the Trig/GB-kit (Roche Diagnostics, Almere, the Netherlands).

T₄ Plasma Clearance

This experiment was conducted in 8- to 18-week-old male and female Oatp1a/1b KO mice, or Oatp1a/1b KO mice reconstituted with human OATP1B1 or OATP1B3 (KO-h1B1 or KO-h1B3) and their respective FVB control animals of the same age and sex. Myrcludex B or placebo was administered subcutaneously. The gallbladder was cannulated, and bile was collected after distal ligation of the common bile duct, as described.^{13,62} Bile was continuously collected with a 10-minute interval for 90 minutes. After the 30-minute bile depletion period, 1- μ Ci [¹²⁵I]T₄ supplemented with equal

Table 1. Primer Sequences Used for Reverse Transcription Quantitative Polymerase Chain Reaction Analysis in Mouse Brown Adipocytes and Liver

Mouse Primers		
36B4	CCAGCGAGGCCACACTGCTG	ACACTGGCCACGTTGCGGAC
HPRT	TTGCTCGAGATGTCATGAAGGA	AGCAGGTCAGCAAAGAACTTATAG
TBP	GGAGAATCATGGACCAGAACA	GATGGGAATTCAGGAGTCA
Ucp1	CAGCTTTGCCTCACTCAGGA	AAGCATTGTAGGTCCCCGTG
Dio1	GTTTGTCTGAAGGTCCGCT	GCCTGCTGCCTGAATGAAATC
Dio2	CTTCTGGCGCTCTATGACTC	CCCCATCAGCGGTCTTCTC
α SMA	ACTACTGCCGAGCGTGAGAT	AAGGTAGACAGCGAAGCCAG
Col1a1	CCCATTGGTAACGTTGGTGC	GGACCTTTGCCCTTCTTT
MCP-1	CTTCTGGGCTGCTGTCA	CCAGCCTACTCATTGGGATCA
TGF- β	CAACCCAGGTCCTTCTAAA	GGAGAGCCCTGGATACCAAC

molar amount of unlabeled T4 in saline was injected via the tail vein, and blood was sampled after 1, 2, 4, 8, 15, 25, 40, and 60 minutes. The experiment was terminated by heart puncture, organs were collected and weighted, and radioactivity was measured by a Wizard2 gamma counter (Perkin Elmer).

Cell Culture and Experiments

The GLUTag mouse intestinal L-cell line (a kind gift from Leslie Glasssmith and Daniel Drucker) was grown in Dulbecco's modified Eagle's medium with low glucose (1 g/L) (Lonza, Basel, Switzerland) supplemented with 10% fetal calf serum (FCS) (Gibco, Gaithersburg, MD), 1% glutamine (Lonza), and 1% penicillin/streptomycin (Lonza). Cells were passaged twice a week at a confluence of 70%–80% and incubated in a humidified atmosphere of 37°C + 5% CO₂. GLP-1 secretion was measured in 24-well plates coated with 1% matrigel, in which the GLUTag cells were seeded 24 hours previously in a medium containing charcoal-treated FCS. On the day of the experiment, cells received fresh complete medium supplemented with 10- μ M, 100- μ M, or 1-mM TCDCa; 1- μ M TC-G 1005; 3- μ M GW4064; or 0.1% DMSO. Supernatant was collected 2 hours later, and GLP-1 was measured by ELISA as described previously. To determine cAMP secretion in GLUTag cells, cells were grown in T75 culture flasks to 80%–90% confluency. Twenty-four hours prior to harvesting the cells, the medium was refreshed for medium supplemented with charcoal-treated FCS. Cells were trypsinized and resuspended at 30×10^6 cells/mL. To each 100- μ L sample, an equal volume of start reagent (complete medium containing 1-mM IBMX) unsupplemented or supplemented with similar components and concentrations as described for the GLP-1 secretion protocol. Additionally, 25- μ M forskolin was added as positive control. After 2 minutes, cAMP accumulation was stopped by immediate lysing of the cells with 200- μ L 2% Triton X-100 in a 0.2-M HCl solution. Samples were incubated for 10 minutes at RT, followed by 10 minutes of centrifugation at 14,000 rpm and at 15°C. A total of 100 μ L of supernatant was used to determine direct cAMP by ELISA, following the manufacturer's instructions (ADI-900-66; Enzo, Farmingdale, NY).

RNA Isolation and Reverse Transcription Quantitative Polymerase Chain Reaction

Total RNA was isolated from approximately 50 mg of tissue with TRI Reagent (Sigma-Aldrich). RNA integrity was assessed spectrophotometrically at 260 nm using a Nanodrop 1000 (Thermo Scientific, Wilmington, DE). One microgram of total RNA was treated with DNase (Promega, Madison, WI) and first-strand complementary DNA was synthesized with Oligo-dT and Revertaid reverse transcriptase (Fermentas, Vilnius, Lithuania). Reverse transcription quantitative polymerase chain reaction was carried out in a Roche Lightcycler 480 II instrument using SensiFAST SYBR No-ROX kit (Bioline, London, United Kingdom) and was analyzed using LinRegPCR 12.5 software (Dr J.M. Ruijter, Amsterdam, The Netherlands).⁶³ Expression levels in each sample were normalized for the geometrical mean of 2 reference genes. Primer sequences are shown in Table 1.

Histopathology and Immunohistochemistry

Formalin-fixed, paraffin-embedded liver or adipose tissue samples (4.5- μ m-thick sections) were stained with hematoxylin (51275; Sigma-Aldrich) and eosin (E4382; Sigma-Aldrich) or Sirius red. Immunohistochemistry for Ki-67 (anti-Ki67 SP6; Thermo Scientific) or UCP-1 (anti-UCP-1) (ab10983; Abcam, Cambridge, United Kingdom) staining were performed as described in Slijepcevic et al.³⁶ From the snap-frozen liver tissue, 5- μ m-thick cryosections were fixed with 3.7% formaldehyde (Sigma-Aldrich) for 60 minutes and stained with Oil Red O (Sigma-Aldrich) for 30 minutes. Digital imaging of all sections was performed using an Olympus BX-51 microscope (Olympus, Tokyo, Japan). The amount of liver fat stained by Oil Red O was calculated from 4 random pictures taken from each cryosection using ImageJ version 1.50i software (National Institutes of Health, Bethesda, MD).

Plasma Biochemistry

Total plasma bile acids and composition were determined by reverse-phase high-performance liquid chromatography as described previously.¹³ Plasma T3 and T4 were measured by in-house radioimmunoassays.⁶⁴ Plasma

biomarkers for liver injury (alanine aminotransferase, aspartate aminotransferase) and cholestatic parameters (ALP) were determined by routine clinical biochemistry testing on a Roche Cobas c502/702 analyzer (Roche Diagnostics, Indianapolis, IN). Total cholesterol and TG content in the main lipoprotein classes (VLDL, low-density lipoprotein, and high-density lipoprotein) was determined using fast protein liquid chromatography. The system contained a PU-980 ternary pump with an LG-980-02 linear degasser, and FP-920 fluorescence and UV-975 UV/VIS detectors (JASCO, Tokyo, Japan). An extra PU-2080i Plus pump (JASCO) was used for in-line cholesterol or TG enzymatic reagent (Roche, Basel, Switzerland) addition at a flowrate of 0.1 mL/min. Plasma lipoproteins were separated using a Superose 6 Increase 10/30 column (GE Healthcare Hoevelaken, the Netherlands) using Tris-buffered saline pH 7.4, as eluent at a flow rate of 0.31 mL/min. Commercially available lipid plasma standards (low, medium, and high) were used for generation of TC or TG calibration curves for the quantitative analysis (SKZL, Nijmegen, the Netherlands) of the separated lipoprotein fractions. Quantitative analysis of the chromatograms was carried out with ChromNAV chromatographic software, version 1.0 (JASCO).

Lipidomics Analysis

Lipidomics analysis was performed as described.⁶⁵ Identification is based on exact mass (with 3 ppm tolerance) and retention time including the relation between these 2 parameters taking into account the different molecular species of the lipid class.⁶⁵ The analysis was performed using the statistical programming language R (R Foundation for Statistical computing version 3.5.2) combined with the ROPLS package.⁶⁶ The Variable Importance in Projection scores estimate the importance of each variable in the projection used in a partial least-squares model and is often used for variable selection. For each variable, the initial *P* value was calculated and corrected for multiple comparisons with the Holm-Sidak method.

Fecal Energy

Energy excreted in feces was measured using a bomb calorimeter (IKA C1; IKA, Staufen, Germany). Feces were compacted and dried in a freeze dryer overnight before combustion.

Statistical Analysis

Data are provided as the mean \pm SE (in vivo experiments) or mean \pm SD (in vitro experiments) of the mean. Differences between 2 groups were analyzed using Student *t* test. One-way analysis of variance with Tukey or Dunnett post hoc analysis was used for multiple group comparisons. Statistical significance was considered at *P* < .05, and calculations and graphs were generated using GraphPad Prism 7.0 (GraphPad Software, San Diego, CA).

References

1. Thomas C, Auwerx J, Schoonjans K. Bile acids and the membrane bile acid receptor TGR5—connecting nutrition and metabolism. *Thyroid* 2008;18:167–174.
2. Fang S, Suh JM, Reilly SM, Yu E, Osborn O, Lackey D, Yoshihara E, Perino A, Jacinto S, Lukasheva Y, Atkins AR, Khvat A, Schnabl B, Yu RT, Brenner DA, Coulter S, Liddle C, Schoonjans K, Olefsky JM, Saltiel AR, Downes M, Evans RM. Intestinal FXR agonism promotes adipose tissue browning and reduces obesity and insulin resistance. *Nat Med* 2015;21:159–165.
3. Pols TW, Nomura M, Harach T, Lo Sasso G, Oosterveer MH, Thomas C, Rizzo G, Gioiello A, Adorini L, Pellicciari R, Auwerx J, Schoonjans K. TGR5 activation inhibits atherosclerosis by reducing macrophage inflammation and lipid loading. *Cell Metab* 2011;14:747–757.
4. Watanabe M, Houten SM, Matakai C, Christoffolete MA, Kim BW, Sato H, Messaddeq N, Harney JW, Ezaki O, Kodama T, Schoonjans K, Bianco AC, Auwerx J. Bile acids induce energy expenditure by promoting intracellular thyroid hormone activation. *Nature* 2006;439:484–489.
5. Holst JJ. The physiology of glucagon-like peptide 1. *Physiol Rev* 2007;87:1409–1439.
6. Pinkney J, Fox T, Ranganath L. Selecting GLP-1 agonists in the management of type 2 diabetes: differential pharmacology and therapeutic benefits of liraglutide and exenatide. *Ther Clin Risk Manag* 2010;6:401–411.
7. Albaugh VL, Banan B, Antoun J, Xiong Y, Guo Y, Ping J, Alikhan M, Clements BA, Abumrad NN, Flynn CR. Role of bile acids and GLP-1 in mediating the metabolic improvements of bariatric surgery. *Gastroenterology* 2019;156:1041–1051.e4.
8. LaRusso NF, Korman MG, Hoffman NE, Hofmann AF. Dynamics of the enterohepatic circulation of bile acids. Postprandial serum concentrations of conjugates of cholic acid in health, cholecystectomized patients, and patients with bile acid malabsorption. *N Engl J Med* 1974;291:689–692.
9. Li T, Holmstrom SR, Kir S, Umetani M, Schmidt DR, Kliewer SA, Mangelsdorf DJ. The G protein-coupled bile acid receptor, TGR5, stimulates gallbladder filling. *Mol Endocrinol* 2011;25:1066–1071.
10. Hodge RJ, Nunez DJ. Therapeutic potential of Takeda-G-protein-receptor-5 (TGR5) agonists. Hope or hype? *Diabetes Obes Metab* 2016;18:439–443.
11. Ali AH, Carey EJ, Lindor KD. Recent advances in the development of farnesoid X receptor agonists. *Ann Transl Med* 2015;3:5.
12. Dawson PA, Lan T, Rao A. Bile acid transporters. *J Lipid Res* 2009;50:2340–2357.
13. Slijepcevic D, Kaufman C, Wichers CG, Gilgioni EH, Lempp FA, Duijst S, de Waart DR, Elferink RP, Mier W, Stieger B, Beuers U, Urban S, van de Graaf SF. Impaired uptake of conjugated bile acids and hepatitis b virus pres1-binding in Na⁺-taurocholate cotransporting polypeptide knockout mice. *Hepatology* 2015;62:207–219.

14. Vaz FM, Paulusma CC, Huidekoper H, de Ru M, Lim C, Koster J, Ho-Mok K, Bootsma AH, Groen AK, Schaap FG, Oude Elferink RP, Waterham HR, Wanders RJ. Sodium taurocholate cotransporting polypeptide (SLC10A1) deficiency: conjugated hypercholanemia without a clear clinical phenotype. *Hepatology* 2015;61:260–267.
15. Hu HH, Liu J, Lin YL, Luo WS, Chu YJ, Chang CL, Jen CL, Lee MH, Lu SN, Wang LY, You SL, Yang HI, Chen CJ, Group R-HS. The rs2296651 (S267F) variant on NTCP (SLC10A1) is inversely associated with chronic hepatitis B and progression to cirrhosis and hepatocellular carcinoma in patients with chronic hepatitis B. *Gut* 2016;65:1514–1521.
16. Ni Y, Lempp FA, Mehrle S, Nkongolo S, Kaufman C, Falth M, Stindt J, Koniger C, Nassal M, Kubitz R, Sultmann H, Urban S. Hepatitis B and D viruses exploit sodium taurocholate co-transporting polypeptide for species-specific entry into hepatocytes. *Gastroenterology* 2014;146:1070–1083.
17. Yan H, Zhong G, Xu G, He W, Jing Z, Gao Z, Huang Y, Qi Y, Peng B, Wang H, Fu L, Song M, Chen P, Gao W, Ren B, Sun Y, Cai T, Feng X, Sui J, Li W. Sodium taurocholate cotransporting polypeptide is a functional receptor for human hepatitis B and D virus. *eLife* 2012;1:e00049.
18. Blank A, Markert C, Hohmann N, Carls A, Mikus G, Lehr T, Alexandrov A, Haag M, Schwab M, Urban S, Haefeli WE. First-in-human application of the novel hepatitis B and hepatitis D virus entry inhibitor myrcludex B. *J Hepatol* 2016;65:483–489.
19. Petersen J, Dandri M, Mier W, Lutgehetmann M, Volz T, von Weizsacker F, Haberkorn U, Fischer L, Pollok JM, Erbes B, Seitz S, Urban S. Prevention of hepatitis B virus infection in vivo by entry inhibitors derived from the large envelope protein. *Nat Biotechnol* 2008;26:335–341.
20. Loglio A, Ferenci P, Colonia Uceda Renteria S, Tham CYL, van Bommel F, Borghi M, Holzmann H, Perbellini R, Trombetta E, Giovanelli S, Greco L, Porretti L, Prati D, Ceriotti F, Lunghi G, Bertoletti A, Lampertico P. Excellent safety and effectiveness of high dose myrcludex-b monotherapy administered for 48 weeks in HDV-related compensated cirrhosis: a case report of 3 patients. *J Hepatol* 2019;71:834–839.
21. Slijepcevic D, Roscam Abbing RLP, Katafuchi T, Blank A, Donkers JM, van Hoppe S, de Waart DR, Tolenaars D, van der Meer JHM, Wildenberg M, Beuers U, Oude Elferink RPJ, Schinkel AH, van de Graaf SFJ. Hepatic uptake of conjugated bile acids is mediated by both sodium taurocholate cotransporting polypeptide and organic anion transporting polypeptides and modulated by intestinal sensing of plasma bile acid levels in mice. *Hepatology* 2017;66:1631–1643.
22. van de Steeg E, Wagenaar E, van der Kruijssen CM, Burggraaff JE, de Waart DR, Elferink RP, Kenworthy KE, Schinkel AH. Organic anion transporting polypeptide 1a/1b-knockout mice provide insights into hepatic handling of bilirubin, bile acids, and drugs. *J Clin Invest* 2010;120:2942–2952.
23. Donkers JM, Appelman MD, van de Graaf SFJ. Mechanistic insights into the inhibition of NTCP by myrcludex B. *JHEP Rep* 2019;1:278–285.
24. Krieger JP, Santos da Conceicao EP, Sanchez-Watts G, Arnold M, Pettersen KG, Mohammed M, Modica S, Lossel P, Morrison SF, Madden CJ, Watts AG, Langhans W, Lee SJ. Glucagon-like peptide-1 regulates brown adipose tissue thermogenesis via the gut-brain axis in rats. *Am J Physiol Regul Integr Comp Physiol* 2018;315:R708–R720.
25. Zhou J, Poudel A, Chandramani-Shivalingappa P, Xu B, Welchko R, Li L. Liraglutide induces beige fat development and promotes mitochondrial function in diet induced obesity mice partially through AMPK-SIRT-1-PGC1-alpha cell signaling pathway. *Endocrine* 2019;64:271–283.
26. Wei Q, Li L, Chen JA, Wang SH, Sun ZL. Exendin-4 improves thermogenic capacity by regulating fat metabolism on brown adipose tissue in mice with diet-induced obesity. *Ann Clin Lab Sci* 2015;45:158–165.
27. Lockie SH, Heppner KM, Chaudhary N, Chabenne JR, Morgan DA, Veyrat-Durebex C, Ananthakrishnan G, Rohner-Jeanrenaud F, Drucker DJ, DiMarchi R, Rahmouni K, Oldfield BJ, Tschop MH, Perez-Tilve D. Direct control of brown adipose tissue thermogenesis by central nervous system glucagon-like peptide-1 receptor signaling. *Diabetes* 2012;61:2753–2762.
28. Bargut TC, Aguila MB, Mandarim-de-Lacerda CA. Brown adipose tissue: updates in cellular and molecular biology. *Tissue Cell* 2016;48:452–460.
29. Cannon B, Nedergaard J. Brown adipose tissue: function and physiological significance. *Physiol Rev* 2004;84:277–359.
30. Kohrle J. The deiodinase family: selenoenzymes regulating thyroid hormone availability and action. *Cell Mol Life Sci* 2000;57:1853–1863.
31. Gereben B, Zavacki AM, Ribich S, Kim BW, Huang SA, Simonides WS, Zeold A, Bianco AC. Cellular and molecular basis of deiodinase-regulated thyroid hormone signaling. *Endocr Rev* 2008;29:898–938.
32. Meyer zu Schwabedissen HE, Ware JA, Finkelstein D, Chaudhry AS, Mansell S, Leon-Ponte M, Strom SC, Zaher H, Schwarz UI, Freeman DJ, Schuetz EG, Tirona RG, Kim RB. Hepatic organic anion transporting polypeptide transporter and thyroid hormone receptor interplay determines cholesterol and glucose homeostasis. *Hepatology* 2011;54:644–654.
33. Hagenbuch B. Cellular entry of thyroid hormones by organic anion transporting polypeptides. *Best Pract Res Clin Endocrinol Metab* 2007;21:209–221.
34. Larsen PR, Zavacki AM. The role of the iodothyronine deiodinases in the physiology and pathophysiology of thyroid hormone action. *Eur Thyroid J* 2012;1:232–242.
35. Kersseboom S, van Gucht ALM, van Mullem A, Brigante G, Farina S, Carlsson B, Donkers JM, van de Graaf SFJ, Peeters RP, Visser TJ. Role of the bile acid transporter SLC10A1 in liver targeting of the lipid-lowering thyroid hormone analog eprotirome. *Endocrinology* 2017;158:3307–3318.

36. Slijepcevic D, Roscam Abbing RLP, Fuchs CD, Haazen LCM, Beuers U, Trauner M, Oude Elferink RPJ, van de Graaf SFJ. Na⁺-taurocholate cotransporting polypeptide inhibition has hepatoprotective effects in cholestasis in mice. *Hepatology* 2018;68:1057–1069.
37. Nie B, Park HM, Kazantzis M, Lin M, Henkin A, Ng S, Song S, Chen Y, Tran H, Lai R, Her C, Maher JJ, Forman BM, Stahl A. Specific bile acids inhibit hepatic fatty acid uptake in mice. *Hepatology* 2012;56:1300–1310.
38. Donkers JM, Kooijman S, Slijepcevic D, Kunst RF, Roscam Abbing RL, Haazen LC, de Waart DR, Levels JH, Schoonjans K, Rensen PC, Oude Elferink RP, Van de Graaf SF. NTCP deficiency in mice protects against obesity and hepatosteatosis. *JCI Insight* 2019;5:127197.
39. Kohli R, Bradley D, Setchell KD, Eagon JC, Abumrad N, Klein S. Weight loss induced by Roux-en-Y gastric bypass but not laparoscopic adjustable gastric banding increases circulating bile acids. *J Clin Endocrinol Metab* 2013;98:E708–E712.
40. Chavez-Talavera O, Baud G, Spinelli V, Daoudi M, Kouach M, Goossens JF, Vallez E, Caiazza R, Ghunaim M, Hubert T, Lestavel S, Tailleux A, Staels B, Pattou F. Roux-en-Y gastric bypass increases systemic but not portal bile acid concentrations by decreasing hepatic bile acid uptake in minipigs. *Int J Obes (Lond)* 2017;41:664–668.
41. Myronovych A, Kirby M, Ryan KK, Zhang W, Jha P, Setchell KD, Dexheimer PJ, Aronow B, Seeley RJ, Kohli R. Vertical sleeve gastrectomy reduces hepatic steatosis while increasing serum bile acids in a weight-loss-independent manner. *Obesity (Silver Spring)* 2014;22:390–400.
42. Hutch CR, Sandoval D. The role of GLP-1 in the metabolic success of bariatric surgery. *Endocrinology* 2017;158:4139–4151.
43. Dirksen C, Damgaard M, Bojsen-Moller KN, Jorgensen NB, Kielgast U, Jacobsen SH, Naver LS, Worm D, Holst JJ, Madsbad S, Hansen DL, Madsen JL. Fast pouch emptying, delayed small intestinal transit, and exaggerated gut hormone responses after Roux-en-Y gastric bypass. *Neurogastroenterol Motil* 2013;25:346–e255.
44. Parker HE, Wallis K, le Roux CW, Wong KY, Reimann F, Gribble FM. Molecular mechanisms underlying bile acid-stimulated glucagon-like peptide-1 secretion. *Br J Pharmacol* 2012;165:414–423.
45. Thomas C, Gioiello A, Noriega L, Strehle A, Oury J, Rizzo G, Macchiarulo A, Yamamoto H, Matakı C, Pruzanski M, Pellicciari R, Auwerx J, Schoonjans K. TGR5-mediated bile acid sensing controls glucose homeostasis. *Cell Metab* 2009;10:167–177.
46. Brighton CA, Rievaj J, Kuhre RE, Glass LL, Schoonjans K, Holst JJ, Gribble FM, Reimann F. Bile acids trigger GLP-1 release predominantly by accessing basolaterally located G protein-coupled bile acid receptors. *Endocrinology* 2015;156:3961–3970.
47. Gonzalez FJ, Jiang C, Patterson AD. An intestinal microbiota-Farnesoid X receptor axis modulates metabolic disease. *Gastroenterology* 2016;151:845–859.
48. De Magalhaes Filho CD, Downes M, Evans RM. Farnesoid X receptor an emerging target to combat obesity. *Dig Dis* 2017;35:185–190.
49. Schumacher JD, Kong B, Pan Y, Zhan L, Sun R, Aa J, Rizzolo D, Richardson JR, Chen A, Goedken M, Aleksunes LM, Laskin DL, Guo GL. The effect of fibroblast growth factor 15 deficiency on the development of high fat diet induced non-alcoholic steatohepatitis. *Toxicol Appl Pharmacol* 2017;330:1–8.
50. Stayrook KR, Bramlett KS, Savkur RS, Ficorilli J, Cook T, Christie ME, Michael LF, Burris TP. Regulation of carbohydrate metabolism by the farnesoid X receptor. *Endocrinology* 2005;146:984–991.
51. Martinez-Augustin O, Sanchez de Medina F. Intestinal bile acid physiology and pathophysiology. *World J Gastroenterol* 2008;14:5630–5640.
52. Werner A, Kuipers F, Verkade HJ. Madame Curie Bioscience Database. Austin, TX: Landes Bioscience, 2000.
53. Galgani J, Ravussin E. Energy metabolism, fuel selection and body weight regulation. *Int J Obes (Lond)* 2008;32(Suppl 7):S109–S119.
54. Bogomolov P, Alexandrov A, Voronkova N, Macievich M, Kokina K, Petrachenkova M, Lehr T, Lempp FA, Wedemeyer H, Haag M, Schwab M, Haefeli WE, Blank A, Urban S. Treatment of chronic hepatitis D with the entry inhibitor myrcludex B: First results of a phase Ib/IIa study. *J Hepatol* 2016;65:490–498.
55. Wedemeyer H, Alexandronov A, Bogomolov P, Blank A, Bremer B, Voronkova N, Schöneweis K, Raupach R, Lehmann P, Darnedde M, Pathil A, Burhenne J, Haag M, Schwab M, Haefeli WE, Urban S. Interim results of a multicenter, open-label phase 2b clinical trial to assess safety an efficacy of Myrcludex B in combination with Tenofovir in patients with chronic HBV/HDV co-infection. *Hepatology* 2017;66:20A–21A.
56. Neuschwander-Tetri BA, Loomba R, Sanyal AJ, Lavine JE, Van Natta ML, Abdelmalek MF, Chalasani N, Dasarathy S, Diehl AM, Hameed B, Kowdley KV, McCullough A, Terrault N, Clark JM, Tonascia J, Brunt EM, Kleiner DE, Doo E, Network NCR. Farnesoid X nuclear receptor ligand obeticholic acid for non-cirrhotic, non-alcoholic steatohepatitis (FLINT): a multicentre, randomised, placebo-controlled trial. *Lancet* 2015;385:956–965.
57. Casaburi I, Avena P, Lanzino M, Sisci D, Giordano F, Maris P, Catalano S, Morelli C, Ando S. Chenodeoxycholic acid through a TGR5-dependent CREB signaling activation enhances cyclin D1 expression and promotes human endometrial cancer cell proliferation. *Cell Cycle* 2012;11:2699–2710.
58. Hong J, Behar J, Wands J, Resnick M, Wang LJ, DeLellis RA, Lambeth D, Souza RF, Spechler SJ, Cao W. Role of a novel bile acid receptor TGR5 in the development of oesophageal adenocarcinoma. *Gut* 2010;59:170–180.
59. Roscam Abbing RLP, Slijepcevic D, Donkers JM, Havinga R, Duijst S, Paulusma CC, Kuiper J, Kuipers F, Groen AK, Oude Elferink RPJ, van de Graaf SFJ. Blocking sodium-taurocholate cotransporting

- polypeptide stimulates biliary cholesterol and phospholipid secretion. *Hepatology* 2020;71:247–258.
60. Li W, Urban S. Entry of hepatitis B and hepatitis D virus into hepatocytes: basic insights and clinical implications. *J Hepatol* 2016;64:S32–S40.
61. Lutgehetmann M, Mancke LV, Volz T, Helbig M, Allweiss L, Bornscheuer T, Pollok JM, Lohse AW, Petersen J, Urban S, Dandri M. Humanized chimeric uPA mouse model for the study of hepatitis B and D virus interactions and preclinical drug evaluation. *Hepatology* 2012;55:685–694.
62. Oude Elferink RP, Ottenhoff R, van Wijland M, Smit JJ, Schinkel AH, Groen AK. Regulation of biliary lipid secretion by mdr2 P-glycoprotein in the mouse. *J Clin Invest* 1995;95:31–38.
63. Ramakers C, Ruijter JM, Deprez RH, Moorman AF. Assumption-free analysis of quantitative real-time polymerase chain reaction (PCR) data. *Neurosci Lett* 2003;339:62–66.
64. Wiersinga WM, Chopra IJ. Radioimmunoassay of thyroxine (T4), 3,5,3'-triiodothyronine (T3), 3,3',5'-triiodothyronine (reverse T3, rT3), and 3,3'-diiodothyronine (T2). *Methods Enzymol* 1982;84:272–303.
65. Herzog K, Pras-Raves ML, Vervaart MA, Luyf AC, van Kampen AH, Wanders RJ, Waterham HR, Vaz FM. Lipidomic analysis of fibroblasts from Zellweger spectrum disorder patients identifies disease-specific phospholipid ratios. *J Lipid Res* 2016;57:1447–1454.
66. Thevenot EA, Roux A, Xu Y, Ezan E, Junot C. Analysis of the human adult urinary metabolome variations with age, body mass index, and sex by implementing a comprehensive workflow for univariate and OPLS statistical analyses. *J Proteome Res* 2015;14:3322–3335.

Received August 20, 2019. Revised April 13, 2020. Accepted April 13, 2020.

Correspondence

Address correspondence to: Stan van de Graaf, Meibergdreef 69-71, 1105 BK Amsterdam, the Netherlands. e-mail: k.f.vandegraaf@amsterdamumc.nl; fax: 020-5669190.

Acknowledgments

The authors thank Suzanne Duijst and Dagmar Tolenaars for helping with the gallbladder cannulations, Ai Lan Souw for helping with the cell culture experiments, Lizette Haazen and Esther Vogels for helping with tissue histology, and Rudi de Waart for the high-performance liquid chromatography measurements. We also thank Leslie Glasssmith and Daniel Drucker for providing the GLUTag cells and Cristina Lebre for breeding and providing several mouse strains.

Conflicts of interest

The authors disclose no conflicts.

Funding

Stan F.J. van de Graaf is supported by the Netherlands Organization for Scientific Research (Vidi; no. 91713319) and the European Research Council (Starting grant no. 337479).